EUROMECH Colloquium 511 on Biomechanics of Human Motion
J. Ambrosio et.al. (eds.)
Ponta Delgada, Azores, Portugal, 9–12 March 2011

DEVELOPMENT OF AN ASYMPTOTIC MODELLING METHODOLOGY FOR TIBIO-FEMORAL CONTACT IN MULTIBODY DYNAMIC SIMULATIONS OF THE HUMAN KNEE JOINT

Ivan Argatov

Institute of Mathematics and Physics, Aberystwyth University, SY23 3BZ Wales, UK
e-mail: iva1@aber.ac.uk

Keywords: Articular contact, Knee joint, Asymptotic modelling, Multibody dynamics.

Abstract. *A new methodology for modelling articular tibio-femoral contact based on the recently developed asymptotic model of frictionless elliptical contact interaction between thin biphasic cartilage layers is presented. The developed mathematical model of articular contact is extended to the case of contact between arbitrary viscoelastic incompressible coating layers. The approach requires use of the smooth contact surface geometry and efficient contact points detection methods. A generalization of the influence surface theory based method for representing articular surfaces from the unstructured noisy surface data is proposed. The normal contact forces are determined analytically based on the exact solution for elliptical contact between thin cartilage layers modelled as viscoelastic incompressible layers. The effective geometrical characteristics of articular surfaces are introduced for using in the developed asymptotic models of elliptical contact between articular surfaces.*

1 INTRODUCTION

Multibody dynamic simulations of joints require modelling of the distributed internal forces generated by articular contact. It is believed that namely dynamic and impact patterns of the contact pressures play an important role in the development and progression of knee joint osteoarthritis [1]. Thus, multibody dynamic models of the knee joint capable of predicting contact stresses would be useful for studying the mechanical aspects of this joint degenerative disease.

In several multibody dynamic models for the tibio-femoral joint [2, 3, 4], the articular contact problem is resolved under the assumption of a rigid contact formulation, when the contact between the surface of each femoral condyle and the surface of the tibia takes place at a single point and no deformation is considered in the articular cartilage layers due to the contact loading. In contrast to the rigid contact model, the deformable contact model, which takes into account deformation of the articular cartilage layers, requires not only a description of the articular surface geometry, but also additional information about the deformation behavior of articular cartilage. As it was observed in [5], the advantage of deformable articular contact model over the rigid contact model is two-fold: 1) It is not restricted to contraform contact, and conforming surfaces can also be considered; 2) It turns out that the knee multibody dynamic model with deformable contact has a higher numerical stability.

A multibody knee contact modelling methodology [6, 7] based on the deformable contact model should include the implementation of an efficient mathematical model for calculating contact pressures and the resulting contact forces. A number of musculoskeletal models of the knee joint employ different forms of the elastic Winkler foundation model [5]. It is known [8] that this model is appropriate for describing the stress-deformation behavior of thin compressible elastic coating layers, and it fails to represent contact interaction of incompressible layers. At the same time, it was shown [9] that the instantaneous response of a biphasic cartilage layer under distributed normal forces is in perfect agreement with the corresponding solution for a bonded thin incompressible elastic layer.

In recent years, finite-element (FE) models have been increasingly used to simulate articular contact [10, 11]. In particular, a mathematical model of distributed contact using a number of contacting patches was employed in [12]. At that, a uniform stress distribution over each contact patch was assumed. The advantage of FE models over the elastic foundation model consists in their ability to evaluate the sub-surface stresses, and these models are not confined to simple geometrical configurations, to which the rigid contact model is restricted. However, as it was observed in [13], in comparison with simple deformable contact models, FE models are too time consuming for the simulation of the knee joint dynamics in real activities such as the gait cycle. Very recently, a novel surrogate modelling approach for performing computationally efficient three-dimensional elastic contact with general surface geometry was proposed in [14] in order to lower the high computational cost of repeated contact analysis within multibody dynamic simulations. The method [14] fits a computationally cheap surrogate contact model to data points sampled from a computationally expensive FE elastic contact model.

A new methodology for modelling tibio-femoral contact presented in this study is based on the recently developed asymptotic model of frictionless elliptical contact interaction between thin biphasic [15] and viscoelastic [16] layers. The approach requires use of the smooth contact surface geometry and efficient contact points detection methods. While the subchondral bone is assumed to be rigid, we study different models for the articular cartilage which is considered to be a thin layer of isotropic linear-elastic or viscoelastic (compressible or incompressible) material. The normal contact forces are determined analytically based on the exact solution for

elliptical contact between thin viscoelastic compressible or incompressible cartilage layers.

As it was observed in [12], an anatomical based multibody dynamics model requires an accurate description of the articular surfaces in order to solve the articular contact problem. In this study, we present a generalization of the method [17] for representing articular surfaces from the unstructured experimental surface data, which can be used for regularization of noisy surface data. Finally, we introduce the effective geometrical characteristics of articular surfaces for using in the developed asymptotic models of elliptical contact between articular surfaces.

2 ARTICULAR SURFACE GEOMETRY

The geometrical data of the tibia and femur are assumed to be given in Cartesian coordinate systems (x_1, x_2, x_3) and $(\hat{x}_1, \hat{x}_2, \hat{x}_3)$, respectively. Following [5], the positive x_1-axis is directed anteriorly, the positive x_2-axis is pointed medially, and the positive x_3-axis is directed proximally (Fig. 1). To describe the relative position of the femur with respect to the tibia, let us assume that the tibia is considered to be rigidly fixed. In such a case, the coordinates $\mathbf{x}$ and $\hat{\mathbf{x}}$ can be referred to as the "space-fixed" and "body-fixed" [18]. We assume that in the fully extended position of the joint, the directions of the corresponding coordinate axes of both coordinate systems coincide.

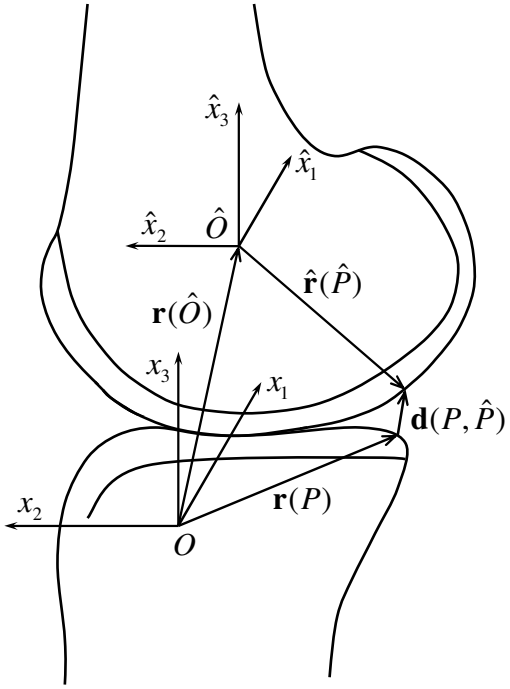

Figure 1: Knee joint coordinate systems.

Let the position of an arbitrary point $\hat{P}$ on the femoral surface is represented by the vector $\hat{\mathbf{r}}(\hat{P})$ in the body-fixed coordinate system. To describe the position vector $\mathbf{r}(\hat{P})$ of the same point in the space-fixed system, one needs the transition vector $\mathbf{r}(\hat{O})$ from the origin of the tibial coordinate system (point O) to the origin of the femoral coordinate system (point $\hat{O}$) and the rotation transformation matrix $\mathcal{R}$ (for its description, see [5]). According to these definitions, the following relation holds [5, 18]:

$$\mathbf{r}(\hat{P}) = \mathbf{r}(\hat{O}) + \mathcal{R}\hat{\mathbf{r}}(\hat{P}). \tag{1}$$

Consider now an arbitrary point P on the tibial surface and a distance vector between the

points P and $\hat{P}$ (see, Fig. 1), i. e.,

$$\mathbf{d}(P,\hat{P}) = \mathbf{r}(\hat{P}) - \mathbf{r}(P). \tag{2}$$

Following [7, 19], we introduce the normal contact distance vector, $\mathbf{d}_0$, between the articular surfaces in such a way that it is parallel to each of the surface normals. The corresponding points P^0 and $\hat{P}^0$ are called the potential contact points. At that, $\mathbf{d}_0 = \mathbf{d}(P^0,\hat{P}^0)$.

The length of vector $\mathbf{d}_0$ with the proper sign taken into account will be called the pseudo-penetration and will be denoted as follows:

$$\delta_0 = -\mathbf{d}_0 \cdot \mathbf{n}^0. \tag{3}$$

Here, $\mathbf{n}^0$ is the outer normal to the tibial surface at the point P^0, and the dot denotes scalar product. We will assume that for any admissible position of the femur relative to the tibia, there is only a pair of the potential contact points P^0 and $\hat{P}^0$ for each pair of femoral and tibial condyles. Note that this assumption is in agreement with the geometric compatibility of rigid bodies condition used in [2, 3, 4]. Therefore, if $\delta_0 = 0$, then the articular surfaces contact each other at a single point. In this case a single tangent plane exists to both femoral and tibial surfaces. If $\mathbf{d}_0 \cdot \mathbf{n}^0 > 0$ (and $\mathbf{d}_0 \cdot \hat{\mathbf{n}}^0 < 0$, where $\hat{\mathbf{n}}^0$ is the outer normal to the femoral surface at the point $\hat{P}^0$), then there is no contact between the surfaces and $\delta_0 < 0$ (see, Fig. 2, a). And finally, the penetration condition states that if $\mathbf{d}_0 \cdot \mathbf{n}^0 < 0$ (and $\mathbf{d}_0 \cdot \hat{\mathbf{n}}^0 > 0$), then the contact between the articular surfaces exists and $\delta_0 > 0$ (see, Fig. 2, b).

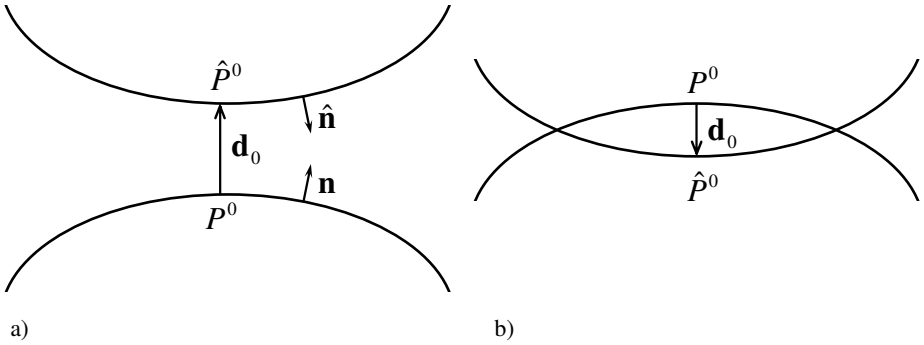

Figure 2: Pseudo-penetration of the contacting bodies.

Furthermore, let us introduce a local Cartesian coordinate system (ξ_1, ξ_2, ζ) with the center at the point P^0 in such a way that the positive ζ-axis points along the normal vector $\mathbf{n}^0$. Locally, that is in the vicinity of points P^0 and $\hat{P}^0$, the equations of both articular surfaces can be written as follows:

$$\zeta = -\phi_0(\boldsymbol{\xi}), \quad \zeta = -\delta_0 + \hat{\phi}_0(\boldsymbol{\xi}). \tag{4}$$

It is assumed that locally the tibia and femur occupy the domains $\zeta \le -\phi_0(\boldsymbol{\xi})$ and $\zeta \ge -\delta_0 + \hat{\phi}_0(\boldsymbol{\xi})$, respectively.

In view of Eqs. (4), we define the local gap function as

$$\phi(\boldsymbol{\xi}) = \phi_0(\boldsymbol{\xi}) + \hat{\phi}_0(\boldsymbol{\xi}). \tag{5}$$

In the next section, following [2], we may assume that the functions $\phi_0(\boldsymbol{\xi})$ and $\hat{\phi}_0(\boldsymbol{\xi})$ can be approximated by polynomials in ξ_1 and ξ_2 of degrees n and $\hat{n}$ as follows:

$$\phi_0(\boldsymbol{\xi}) = \sum_{p=2}^{n}\sum_{q=0}^{p} a_{pq}\xi_1^{p-q}\xi_2^{q}, \quad \hat{\phi}_0(\boldsymbol{\xi}) = \sum_{p=2}^{\hat{n}}\sum_{q=0}^{p} \hat{a}_{pq}\xi_1^{p-q}\xi_2^{q}. \tag{6}$$

The coefficients a_{pq} and $\hat{a}_{pq}$ are calculated by minimizing the functions

$$\sum_{j=1}^{N}\Big(\zeta^j - \sum_{p=2}^{n}\sum_{q=0}^{p} a_{pq}(\xi_1^j)^{p-q}(\xi_2^j)^q\Big)^2, \quad \sum_{j=1}^{\hat{N}}\Big(\hat{\zeta}^j - \sum_{p=2}^{\hat{n}}\sum_{q=0}^{p} \hat{a}_{pq}(\hat{\xi}_1^j)^{p-q}(\hat{\xi}_2^j)^q\Big)^2, \tag{7}$$

where N and $\hat{N}$ are the numbers of measured surface points, and $(\xi_1^j, \xi_2^j, \zeta^j)$ and $(\hat{\xi}_1^j, \hat{\xi}_2^j, \hat{\zeta}^j)$ are the measured coordinates of the j-th point on the tibial surface ($j = 1, \ldots, N$) and on the femoral surface ($j = 1, \ldots, \hat{N}$), respectively.

3 CONTACT CONSTITUTIVE RELATIONS

3.1 Elastic foundation model. Elliptical contact of thin compressible elastic layers

Consider a frictionless contact between two thin linear elastic layers of constant thicknesses, h_1 and h_2, firmly attached to rigid substrates with continuously varying curvatures. Let us assume that in the undeformed state, the surfaces of the layers touch at a single point denoted by P^0. Introducing a Cartesian coordinate system (η_1, η_2, ζ) with the center at the point P^0 such that the coordinate plane $\zeta = 0$ coincides with the common tangent plane to the layer surfaces, without loss of generality, we may assume that with the accuracy up to terms of order $|\boldsymbol{\eta}|^3$ the gap function, $\varphi(\boldsymbol{\eta})$, defined as the distance between the layer surfaces along the ζ-axis, is represented by an elliptic paraboloid

$$\varphi(\boldsymbol{\eta}) = (2R_1)^{-1}\eta_1^2 + (2R_2)^{-1}\eta_2^2. \tag{8}$$

Let $w(\boldsymbol{\eta})$ and $\hat{w}(\boldsymbol{\eta})$ be the vertical displacement functions for the surface points of the layers representing the tibial and femoral articular cartilages, respectively, due to the action of the surface pressures $p(\boldsymbol{\eta})$. Given that the materials of the layers are elastic with Young's moduli E_1 and E_2, and Poisson's ratios ν_1 and ν_2, which are assumed to be not too close to 0.5, we will have

$$w(\boldsymbol{\eta}) = -E_1^{-1}\tilde{\mathcal{A}}_1 h_1 p(\boldsymbol{\eta}), \quad \hat{w}(\boldsymbol{\eta}) = E_2^{-1}\tilde{\mathcal{A}}_2 h_2 p(\boldsymbol{\eta}). \tag{9}$$

Here the index 1 refers to the tibia and 2 refers to the femur, and the following notation is used:

$$\tilde{\mathcal{A}}_n = \frac{(1+\nu_n)(1-2\nu_n)}{1-\nu_n}. \tag{10}$$

Let also δ_0 be the vertical approach of the rigid substrates. Then, the following equation should hold in the contact region, ω, where the contact pressure is positive:

$$\hat{w}(\boldsymbol{\eta}) - w(\boldsymbol{\eta}) = \delta_0 - \varphi(\boldsymbol{\eta}), \quad \boldsymbol{\eta} \in \omega. \tag{11}$$

Substituting the expressions (9) into Eq. (11), we obtain the contact condition in the form

$$\big(E_1^{-1}\tilde{\mathcal{A}}_1 h_1 + E_2^{-1}\tilde{\mathcal{A}}_2 h_2\big)p(\boldsymbol{\eta}) = \delta_0 - \varphi(\boldsymbol{\eta}). \tag{12}$$

From Eq. (12), it immediately follows that

$$p(\boldsymbol{\eta}) = k\big(\delta_0 - \varphi(\boldsymbol{\eta})\big), \tag{13}$$

where k is the Winkler foundation modulus given by

$$k = \left(\frac{(1+\nu_1)(1-2\nu_1)h_1}{(1-\nu_1)E_1} + \frac{(1+\nu_2)(1-2\nu_2)h_2}{(1-\nu_2)E_2}\right)^{-1}. \tag{14}$$

It is obvious that if the layers' materials are similar (i. e., $E_1 = E_2 = E$ and $\nu_1 = \nu_2 = \nu$), formula (14) simplifies to the following one:

$$k = \frac{(1-\nu)E}{(1+\nu)(1-2\nu)h}. \tag{15}$$

Here, $h = h_1 + h_2$ is the joint thickness.

Integrating the contact pressure distribution (13) over the contact region ω, we obtain the contact force

$$P = \iint\limits_{\omega} p(\boldsymbol{\eta})\, d\boldsymbol{\eta}. \tag{16}$$

In the case of a paraboloidal gap function (8), in view of (13), we find that the contact area ω is an elliptical domain with the semi-axes $a = \sqrt{2R_1\delta_0}$ and $b = \sqrt{2R_2\delta_0}$. According to Eqs. (8), (13), and (16), we will have

$$P = \pi k\sqrt{R_1R_2}\delta_0^2. \tag{17}$$

Eq. (17) represents the force-displacement relationship for the case of elliptical contact of thin compressible coatings. The fact that a thin elastic layer with its Poisson's ratio not too close to 0.5 behaves like a Winkler elastic foundation was first rigorously established in [20]. The case of elliptical contact in the framework of elastic foundation model was considered in detail in [21]. The elastic foundation model based on Eq. (15) was used for multibody dynamic simulations of knee contact mechanics in a number of papers [5, 22]. Formula (14) was recently considered in [13]. A discussion of analytical models employed for describing articular contact is presented in [13] along with a comparative study of four different models: the classical Hertz contact model, Elastic foundation model, a new modified elastic foundation model, which takes into account the Hertzian type contact for relatively low conforming surfaces and small contact areas, and the finite-element model.

3.2 Asymptotic model for elliptical contact of thin incompressible elastic layers

It is readily seen that the coefficient $\tilde{\mathcal{A}}_n$ defined by formula (10) vanishes as $\nu_n \to 0.5$, and consequently the Winkler foundation modulus k tends to infinity (see, Eqs. (14), (15)).

Based on the asymptotic analysis of the frictionless contact problem for a thin elastic layer bonded to a rigid substrate in the thin-layer limit [23], the following contact constitutive relations for thin incompressible layers can be established instead of Eqs. (9):

$$w(\boldsymbol{\eta}) = -E_1^{-1}\tilde{\mathcal{B}}_1 h_1^3 \Delta p(\boldsymbol{\eta}), \quad \hat{w}(\boldsymbol{\eta}) = E_2^{-1}\tilde{\mathcal{B}}_2 h_2^3 \Delta p(\boldsymbol{\eta}). \tag{18}$$

Here, $\Delta = \partial^2/\partial\eta_1^2 + \partial^2/\partial\eta_2^2$ is the Laplace differential operator, and

$$\tilde{\mathcal{B}}_n = \frac{\nu_n(1+\nu_n)(4\nu_n-1)}{3(1-\nu_n)^2}. \tag{19}$$

Substituting the expressions (18) into the contact condition (11), we obtain

$$-\big(E_1^{-1}\tilde{\mathcal{B}}_1 h_1^3 + E_2^{-1}\tilde{\mathcal{B}}_2 h_2^3\big)\Delta p(\boldsymbol{\eta}) = \delta_0 - \varphi(\boldsymbol{\eta}). \tag{20}$$

Eq. (20) should hold over the whole contact region ω. According to [8, 24], we impose the following boundary conditions on the contour Γ of the contact region ω:

$$p(\boldsymbol{\eta}) = 0, \quad \frac{\partial p}{\partial n}(\boldsymbol{\eta}) = 0, \quad \boldsymbol{\eta} \in \Gamma. \tag{21}$$

Here, $\partial/\partial n$ is the normal derivative.

In the case of a paraboloidal gap function (8), the exact solution to the problem (20), (21) was obtained in [8] in the form

$$p(\boldsymbol{\eta}) = p_0\left(1 - \frac{\eta_1^2}{a^2} - \frac{\eta_2^2}{b^2}\right)^2. \tag{22}$$

The maximum contact pressure p_0 and the semi-axes a and b of the elliptical contact region ω satisfy the following system of algebraic equations [8]:

$$\delta_0 = \frac{4p_0}{m}\left(\frac{1}{a^2} + \frac{1}{b^2}\right), \tag{23}$$

$$\frac{1}{2R_1} = \frac{4p_0}{ma^2}\left(\frac{3}{a^2} + \frac{1}{b^2}\right), \quad \frac{1}{2R_2} = \frac{4p_0}{mb^2}\left(\frac{1}{a^2} + \frac{3}{b^2}\right). \tag{24}$$

Here we introduced the notation

$$m = \left(E_1^{-1}\tilde{\mathcal{B}}_1 h_1^3 + E_2^{-1}\tilde{\mathcal{B}}_2 h_2^3\right)^{-1}. \tag{25}$$

If the layers' materials are similar, formula (25) simplifies to the following one:

$$m = \frac{3(1-\nu^2)^2 E}{\nu(4\nu-1)(1+\nu)(h_1^3 + h_2^3)}. \tag{26}$$

Integrating the contact pressure distribution (22) over the contact region ω and taking into account Eqs. (16), (23), and (24), we obtain the force-displacement relationship

$$P = \frac{\pi m}{3} M_P(s) R_1 R_2 \delta_0^3. \tag{27}$$

Here, $s = b/a$ is the aspect ratio of the contact area, and the factor $M_P(s)$ is given by

$$M_P(s) = \frac{s(3s^2+1)(s^2+3)}{(s^2+1)^3}. \tag{28}$$

According to Eqs. (24), the following relation holds true [15]:

$$s^2 = \sqrt{\left(\frac{R_1 - R_2}{6R_1}\right)^2 + \frac{R_2}{R_1}} - \frac{(R_1 - R_2)}{6R_1}. \tag{29}$$

Eq. (27) represents the force-displacement relationship for the case of elliptical contact of thin incompressible coatings.

3.3 Asymptotic model for elliptical contact of thin compressible viscoelastic layers

For the sake of simplicity, we assume that Poisson's ratios ν_1 and ν_2 of the viscoelastic layers are time independent. Then, applying the viscoelastic correspondence principle to the associated elastic equation (12), one arrives at the following governing integral equation:

$$\frac{h}{E_\infty}\int_{0-}^{t} \Phi_\alpha(t-\tau)\frac{\partial p}{\partial \tau}(\boldsymbol{\eta},\tau)\,d\tau = \delta_0(t) - \varphi(\boldsymbol{\eta})\mathcal{H}(t). \tag{30}$$

Here, $\delta_0(t)$ is the variable approach of the rigid substrates, t is a time variable, $\mathcal{H}(t)$ is the Heaviside step function such that $\mathcal{H}(t) = 1$ for $t > 0$ and $\mathcal{H}(t) = 0$ for $t \le 0$, E_∞ is a harmonic mean of the relaxed elastic moduli E_1^∞ and E_2^∞, $\Phi_\alpha(t)$ is the compound creep function, i. e.,

$$\Phi_\alpha(t) = \alpha_1\Phi_1(t) + \alpha_2\Phi_2(t),$$

$$E_\infty = \frac{2E_1^\infty E_2^\infty}{E_1^\infty + E_2^\infty}, \quad \alpha_1 = \frac{2E_2^\infty h_1\widetilde{\mathcal{A}}_1}{(E_1^\infty + E_2^\infty)(h_1+h_2)}, \quad \alpha_2 = \frac{2E_1^\infty h_2\widetilde{\mathcal{A}}_2}{(E_1^\infty + E_2^\infty)(h_1+h_2)}.$$

Recall that the constants $\widetilde{\mathcal{A}}_1$ and $\widetilde{\mathcal{A}}_2$ are defined by formula (10).

The force-displacement relationship is given be the following equation [16]:

$$P(t) = \frac{\pi}{h}\sqrt{R_1R_2}E_\infty \int\limits_{0-}^{t} \Psi_\alpha(t-\tau)\frac{d}{d\tau}\big(\delta_0^2(\tau)\big)\,d\tau. \tag{31}$$

Here, $\Psi_\alpha(t)$ is the compound relaxation function determined by the relaxation functions $\Psi_1(t)$ and $\Psi_2(t)$ of the viscoelastic compressible coatings as follows:

$$\Psi_\alpha(t) = \frac{1}{\alpha_1}\Psi_1(t) + \frac{1}{\alpha_2}\Psi_2(t).$$

Note that if the layer's materials follow a standard linear viscoelastic solid model, we have

$$\Phi_n(t) = 1 - (1-\rho_n)\exp(-t/T_n),$$

$$\Psi_n(t) = 1 - (1-1/\rho_n)\exp(-t/(\rho_n T_n)),$$

where T_n is the characteristic relaxation time of strain under applied step of stress, $\rho_n = E_n^\infty/E_n^0$ is the ratio of E_n^∞ to the unrelaxed elastic modulus E_n^0.

3.4 Asymptotic model for elliptical contact of thin incompressible viscoelastic layers

Applying the viscoelastic correspondence principle to the associated elastic equation (20), we arrive at the following governing integro-differential equation:

$$-\frac{h^3}{E_\infty}\int\limits_{0-}^{t} \Phi_\beta(t-\tau)\Delta\frac{\partial p}{\partial\tau}(\boldsymbol{\eta},\tau)\,d\tau = \delta_0(t) - \varphi(\boldsymbol{\eta})\mathcal{H}(t). \tag{32}$$

Here, $\Delta = \partial^2/\partial\eta_1^2 + \partial^2/\partial\eta_2^2$ is the Laplace operator, $\Phi_\beta(t)$ is the compound creep function determined by the formulas

$$\Phi_\beta(t) = \beta_1\Phi_1(t) + \beta_2\Phi_2(t),$$

$$\beta_1 = \frac{2E_2^\infty h_1^3\widetilde{\mathcal{B}}_1(\nu_1)}{(E_1^\infty + E_2^\infty)(h_1+h_2)^3}, \quad \beta_2 = \frac{2E_1^\infty h_2^3\widetilde{\mathcal{B}}_2(\nu_2)}{(E_1^\infty + E_2^\infty)(h_1+h_2)^3}.$$

At that, the constants $\widetilde{\mathcal{B}}_1$ and $\widetilde{\mathcal{B}}_2$ are defined by formula (19). As before, we require that the contact pressure distribution $p(\boldsymbol{\eta},t)$ should satisfy the boundary conditions (21).

The general solution of Eq. (32) in the case (8) was derived in [16]. Integrating the obtained contact pressures over the elliptical contact region, we arrive at the following equation:

$$P(t) = \frac{\pi m}{3}M_P(s)R_1R_2\int\limits_{0-}^{t} \Psi_\alpha(t-\tau)\frac{d}{d\tau}\big(\delta_0^3(\tau)\big)\,d\tau. \tag{33}$$

Here, $M_P(s)$ is the factor defined by formula (28), and $\Psi_\beta(t)$ is the compound relaxation function for the viscoelastic incompressible coatings given by

$$\Psi_\beta(t) = \frac{1}{\beta_1}\Psi_1(t) + \frac{1}{\beta_2}\Psi_2(t).$$

It should be noted that Eqs. (31) and (33) are valid for the case of contact interaction consisting of a monotonic loading phase and a monotonic unloading phase. Thus, they can be applied for modelling contact forces in impact situations. We underline that the case of repetitive loading requires a special treatment.

4 EFFECTIVE GEOMETRICAL CHARACTERISTICS OF ARTICULAR CONTACT

4.1 Analytical approximations for articular contact surfaces

To model the articular contact, one needs to describe the articular surface geometry in the framework of a certain mathematical model. A number of surface-fitting methods for representing the three-dimensional topography of articular surfaces, and in particular, B-spline method [25, 26], use a structured data set and provide a limited continuity of the fitted articular surface. Methods to represent articular surfaces from the unstructured data were suggested in [27, 28] and are based on a parametric polynomial representation.

A method for the representation of articular surfaces, which can be effectively deal with non-ordered data points, was introduced in [17] based on the influence surface theory of elastic plates. A set of $N \geq 3$ points $(\boldsymbol{\xi}^j, \zeta^j)$ $(j = 1, \ldots, N)$ is approximated with the function

$$w(\boldsymbol{\xi}) = b_0 + b_1\xi_1 + b_2\xi_2 + \sum_{k=1}^{N} f_k|\boldsymbol{\xi} - \boldsymbol{\xi}^k|^2 \ln|\boldsymbol{\xi} - \boldsymbol{\xi}^k|, \tag{34}$$

where $|\boldsymbol{\xi}| = \sqrt{\xi_1^2 + \xi_2^2}$. For $N + 3$ coefficients $f_1, \ldots, f_N$, b_0, b_1, and b_2, we have the following system of $N + 3$ linear algebraic equations:

$$b_0 + b_1\xi_1^j + b_2\xi_2^j + \sum_{k=1}^{N} f_k|\boldsymbol{\xi}^j - \boldsymbol{\xi}^k|^2 \ln|\boldsymbol{\xi}^j - \boldsymbol{\xi}^k| = \zeta^j, \quad j = 1, \ldots, N, \tag{35}$$

$$\sum_{k=1}^{N} f_k = 0, \quad \sum_{k=1}^{N} \xi_1^k f_k = 0, \quad \sum_{k=1}^{N} \xi_2^k f_k = 0. \tag{36}$$

It is clear that the method [17] provides unlimited continuity of the fitted articular surface (with exception of the data points, where the function (34) is only continuously differentiable).

Since experimental measurements of surface data always contain a degree of measurement uncertainty, it was observed in [25] that a surface-fitting method which consists of interpolating the measured surface data may result in some degree of surface roughness. In [17], it was also noted that one limitation of the fitting method (34) – (36) is that it requires the fitting surface to pass through all measured surface points. This means that the fitting accuracy of the method [17] is partially controlled by the accuracy of the measurement instrument. At that, because of the noise nature of measured data, forcing the fitting surface to pass through all measured surface data points may not produce an optimal fitting surface.

In view of the observation made above, we propose the following regularization of the method [17]. Given the measured surface data points $(\boldsymbol{\xi}^j, \zeta^j)$ $(j = 1, 2, \ldots, N)$, the fitting

surface must satisfy the optimization criterion

$$\min_{f_1,\ldots,f_N,b_0,b_1,b_2} \frac{1}{2}\sum_{j=1}^{N} f_j\Big(b_0+b_1\xi_1^j+b_2\xi_2^j+\sum_{k=1}^{N} f_k|\boldsymbol{\xi}^j-\boldsymbol{\xi}^k|^2\ln|\boldsymbol{\xi}^j-\boldsymbol{\xi}^k|\Big) \tag{37}$$

subject to Eqs. (36) and the unilateral constraint

$$\frac{1}{N}\sum_{j=1}^{N}\Big(b_0+b_1\xi_1^j+b_2\xi_2^j+\sum_{k=1}^{N} f_k|\boldsymbol{\xi}^j-\boldsymbol{\xi}^k|^2\ln|\boldsymbol{\xi}^j-\boldsymbol{\xi}^k|-\zeta^j\Big)^2\le\epsilon^2. \tag{38}$$

Here, ϵ represents a given tolerance level. Now, the approximation (34) will not necessarily pass through the set of surface data points $(\boldsymbol{\xi}^j,\zeta^j)$ $(j=1,2,\ldots,N)$, but it will minimize the plate potential energy (37), while simultaneously keeping the sum of squired distances $\big(w(\boldsymbol{\xi}^j)-\zeta^j\big)^2$ under the given tolerance level.

Note that spline smoothing methods for regularization of noisy data were considered in [25].

4.2 Effective geometrical characteristics in the case of thin compressible layers

In order to apply the force displacement relationship (17) or (31), one needs to evaluate the geometric parameters R_1 and R_2 appearing in the paraboloid approximation (8) of the local gap function (5). In other words, the local gap function (5) must be approximated as follows:

$$\phi(\boldsymbol{\xi})=\varphi(\boldsymbol{\xi})+\tilde{\varphi}(\boldsymbol{\xi}), \tag{39}$$

where $\tilde{\varphi}(\boldsymbol{\xi})$ is in a sense a small discrepancy, while $\varphi(\boldsymbol{\xi})$, according to (8), should be taken in the form

$$\varphi(\boldsymbol{\xi})=\xi_1^2\left(\frac{\cos^2\theta}{2R_1}+\frac{\sin^2\theta}{2R_2}\right)+\xi_2^2\left(\frac{\sin^2\theta}{2R_1}+\frac{\cos^2\theta}{2R_2}\right)+\xi_1\xi_2\sin 2\theta\left(\frac{1}{2R_1}-\frac{1}{2R_2}\right). \tag{40}$$

Observe that the angle θ introduced in (40) has the meaning of the angle between the positive ξ_1-axis and the positive η_1-axis.

Considering the contact problem for the gap function (39) in the framework of the elastic foundation model, we will have the following contact pressure and contact force (see, Eqs. (13) and (16)):

$$p(\boldsymbol{\xi})=k\big(\delta_0-\varphi(\boldsymbol{\xi})-\tilde{\varphi}(\boldsymbol{\xi})\big), \tag{41}$$

$$P=k\iint\limits_{\tilde{\omega}}\big(\delta_0-\varphi(\boldsymbol{\xi})-\tilde{\varphi}(\boldsymbol{\xi})\big)\,d\boldsymbol{\xi}. \tag{42}$$

Here, $\tilde{\omega}$ is the new contact region that somehow slightly differs from the elliptical contact region ω corresponding to the gap function $\varphi(\boldsymbol{\xi})$.

Under the assumption that the gap variation $\tilde{\varphi}(\boldsymbol{\xi})$ introduces a small variation into the contact region ω and the contact force P, we may use the approximate relationship

$$P=k\iint\limits_{\omega}\big(\delta_0-\varphi(\boldsymbol{\xi})\big)\,d\boldsymbol{\xi}. \tag{43}$$

Consequently, according to (39), (42), and (43), the following approximate equation holds:

$$\iint\limits_{\omega} \big(\phi(\boldsymbol{\xi}) - \varphi(\boldsymbol{\xi})\big)\, d\boldsymbol{\xi} = 0. \tag{44}$$

Thus, in view of (44), we suggest the following optimization criterion for choosing the parameters R_1 and R_2:

$$\min_{R_1,R_2,\theta} \iint\limits_{\omega_*} |\phi(\boldsymbol{\xi}) - \varphi(\boldsymbol{\xi})|\, d\boldsymbol{\xi}. \tag{45}$$

Here, ω_* is a characteristic area. In particular, the domain ω_* should contain a maximum contact area for a class of admissible contact loadings. Note that an estimate for ω_* can be obtained based on a polynomial approximation for $\phi(\boldsymbol{\xi})$ (see, Eqs. (5) and (6)). Furthermore, because of the fact that the gap function depends on the orientation of the femur with respect to the tibia, and the aspect ratio of the contact zone changes with this orientation, in the place of ω_* one can substitute a circular domain, which surrounds the maximum elliptical contact zone for all admissible orientations and contact loadings. Finally, observe that the shape of the local gap function $\phi(\boldsymbol{\xi})$ outside of the contact area does not play any role in evaluating the contact pressure and contact force.

4.3 Effective geometrical characteristics in the case of thin incompressible layers

Considering now the contact problem for the gap function (39) in the framework of the asymptotic model for incompressible elastic layers, we will have the following problem for the contact pressure (see, Eqs. (20), (21), and (25)):

$$-m^{-1}\Delta p(\boldsymbol{\xi}) = \delta_0 - \varphi(\boldsymbol{\xi}) - \tilde{\varphi}(\boldsymbol{\xi}), \quad \boldsymbol{\xi} \in \tilde{\omega}, \tag{46}$$

$$p(\boldsymbol{\xi}) = 0, \quad \frac{\partial p}{\partial n}(\boldsymbol{\xi}) = 0, \quad \boldsymbol{\xi} \in \tilde{\Gamma}. \tag{47}$$

Here, $\tilde{\Gamma}$ is the contour of the contact domain $\tilde{\omega}$.

Under the assumption that the gap variation $\tilde{\varphi}(\boldsymbol{\xi})$ introduces a small variation into the elliptical contact region ω corresponding to the gap function $\varphi(\boldsymbol{\xi})$, we derive from Eqs. (46) and (47) the following limit problem for the variation of the contact pressure:

$$m^{-1}\Delta \tilde{p}(\boldsymbol{\xi}) = \tilde{\varphi}(\boldsymbol{\xi}), \quad \boldsymbol{\xi} \in \omega, \tag{48}$$

$$\tilde{p}(\boldsymbol{\xi}) = 0, \quad \frac{\partial \tilde{p}}{\partial n}(\boldsymbol{\xi}) = 0, \quad \boldsymbol{\xi} \in \Gamma. \tag{49}$$

Moreover, the gap variation $\tilde{\varphi}(\boldsymbol{\xi})$ will not greatly influence the resulting contact force, if

$$\iint\limits_{\omega} \tilde{p}(\boldsymbol{\xi})\, d\boldsymbol{\xi} = 0. \tag{50}$$

Applying the second Green's formula and taking into account Eqs. (48) and (49), we reduce Eq. (50) to the following one:

$$\iint\limits_{\omega} (\xi_1^2 + \xi_2^2)\tilde{\varphi}(\boldsymbol{\xi})\, d\boldsymbol{\xi} = 0. \tag{51}$$

Thus, in view of (51), we suggest the following optimization criterion for determining the parameters R_1 and R_2 (compare with (45)):

$$\min_{R_1,R_2,\theta} \iint\limits_{\omega_*} (\phi(\boldsymbol{\xi}) - \varphi(\boldsymbol{\xi}))^2 d\boldsymbol{\xi}. \tag{52}$$

Indeed, two of the three necessary optimality conditions for (52) have the form

$$\iint\limits_{\omega_*} (\phi(\boldsymbol{\xi}) - \varphi(\boldsymbol{\xi}))(\xi_1^2 \cos\theta + \xi_2^2 \sin\theta + \xi_1\xi_2 \sin 2\theta)\, d\boldsymbol{\xi} = 0,$$

$$\iint\limits_{\omega_*} (\phi(\boldsymbol{\xi}) - \varphi(\boldsymbol{\xi}))(\xi_1^2 \sin\theta + \xi_2^2 \cos\theta - \xi_1\xi_2 \sin 2\theta)\, d\boldsymbol{\xi} = 0.$$

Now, adding the equations above, we readily obtain

$$\iint\limits_{\omega_*} (\phi(\boldsymbol{\xi}) - \varphi(\boldsymbol{\xi}))(\xi_1^2 + \xi_2^2)\, d\boldsymbol{\xi} = 0. \tag{53}$$

In other words, Eq. (53) is a necessary optimality condition for (52).

Comparing Eqs. (51) and (53), in view of Eq. (39), we come to the conclusion that Eq. (51) and (53) coincide if their integration domains coincide. This motivates the choice of the optimization criterion (52).

4.4 Determining the effective geometrical characteristics from experimental surface data

The optimization criteria (45) and (52) can be written as

$$\min_{R_1,R_2,\theta} \iint\limits_{\omega_*} |\phi(\boldsymbol{\xi}) - \varphi(\boldsymbol{\xi})|^\sigma d\boldsymbol{\xi}, \tag{54}$$

where $\sigma = 1$ in the case (45) and $\sigma = 2$ in the case (52).

The optimization criterion (54) requires a continuous representation of the gap function $\phi(\boldsymbol{\xi})$, while originally only the coordinates of experimental surface data points $(\xi_1^j, \xi_2^j, \zeta^j)$ $(j = 1, \ldots, N)$ and $(\hat{\xi}_1^j, \hat{\xi}_2^j, \hat{\zeta}^j)$ $(j = 1, \ldots, \hat{N})$ have been provided from the measurement experiment (see, Eq. (7)). For instance, the analytical approximation (34) can be sued. However, it would be useful to have a possibility to determine the parameters R_1 and R_2 directly from the experimental surface data. That is why, the following discrete variant of the optimization criterion (54) makes sense.

Given the measured surface data points $(\xi_1^j, \xi_2^j, \zeta^j)$ $(j = 1, \ldots, N)$ and $(\hat{\xi}_1^j, \hat{\xi}_2^j, \hat{\zeta}^j)$ $(j = 1, \ldots, \hat{N})$, the two sets of effective geometrical parameters R_1^0, R_2^0, θ_0 and $\hat{R}_1^0$, $\hat{R}_2^0$, $\hat{\theta}_0$ must satisfy the criteria

$$\min_{R_1^0,R_2^0,\theta_0} \sum_{\boldsymbol{\xi}^j \in \omega_*} |\zeta^j - \varphi^0(\boldsymbol{\xi}^j)|^\sigma, \tag{55}$$

$$\min_{\hat{R}_1^0,\hat{R}_2^0,\hat{\theta}_0} \sum_{\hat{\boldsymbol{\xi}}^j \in \omega_*} |\hat{\zeta}^j - \hat{\varphi}^0(\hat{\boldsymbol{\xi}}^j)|^\sigma, \tag{56}$$

where $\varphi^0(\boldsymbol{\xi})$ and $\hat{\varphi}^0(\boldsymbol{\xi})$ are given by

$$\varphi^0(\boldsymbol{\xi}) = \xi_1^2\left(\frac{\cos^2\theta_0}{2R_1^0} + \frac{\sin^2\theta_0}{2R_2^0}\right) + \xi_2^2\left(\frac{\sin^2\theta_0}{2R_1^0} + \frac{\cos^2\theta_0}{2R_2^0}\right) + \xi_1\xi_2\sin 2\theta_0\left(\frac{1}{2R_1^0} - \frac{1}{2R_2^0}\right), \quad (57)$$

$$\hat{\varphi}^0(\boldsymbol{\xi}) = \xi_1^2\left(\frac{\cos^2\hat{\theta}_0}{2\hat{R}_1^0} + \frac{\sin^2\hat{\theta}_0}{2\hat{R}_2^0}\right) + \xi_2^2\left(\frac{\sin^2\hat{\theta}_0}{2\hat{R}_1^0} + \frac{\cos^2\hat{\theta}_0}{2\hat{R}_2^0}\right) + \xi_1\xi_2\sin 2\hat{\theta}_0\left(\frac{1}{2\hat{R}_1^0} - \frac{1}{2\hat{R}_2^0}\right). \quad (58)$$

According to (55) and (56), the tibial and femoral surfaces are represented locally by the effective elliptic paraboloids (57) and (58), whose orientations with respect to the positive ξ_1-axis is determined by the angles θ_0 and $\hat{\theta}_0$, respectively. Now, the effective geometrical parameters R_1 and R_2 appearing in the elliptic paraboloidal approximation (8) can be determined from R_1^0, R_2^0, θ_0 and $\hat{R}_1^0$, $\hat{R}_2^0$, $\hat{\theta}_0$ following a standard procedure used in the Hertzian contact mechanics [21].

5 DISCUSSION AND CONCLUSIONS

The asymptotic methodology for tibio-femoral articular contact developed in this paper is based on an asymptotic theory for a thin compressible or incompressible viscoelastic layer attached to a rigid substrate. As it was shown in [16], the viscoelastic contact model for incompressible layers incorporates the asymptotic model [9, 29, 15] for short-time response of biphasic layers as a special case, corresponding to the Maxwell model of viscoelastic material.

In the case of elastic layers, the contact constitutive relations can be represented as follows (see, Eqs. (17) and (27)):

$$P = EMR^l\delta_0^n. \quad (59)$$

Here, E is Young's elastic modulus, $R = \sqrt{R_1R_2}$ is a geometric mean of the curvature radii R_1 and R_2, the factor M is a function of the thicknesses of the layers h_1 and h_2, Poisson's ratio ν, and the aspect ratio s of the elliptical contact region. At that, for compressible layers, $n = 2$ and $l = 1$, while for incompressible layers, $n = 3$ and $l = 2$. Note that the dimension of M is L^{2-n-l}, where L is the dimension of length. Eq. (59) was used in a number of publications on multibody simulations [30]. In particular, it incorporates the Hertzian force-displacement relationship with $n = 3/2$ and $l = 1/2$.

From Eq. (59) (see also, Eqs. (26) and (27)), it is readily seen that in the case of incompressible layers, the contact force, P, is inversely proportional to the joint thickness cubed, h^3, while in the case of thin compressible coatings, the contact force is simply inversely proportional to the joint thickness (see, Eqs. (15) and (17)). This implication is very important from the viewpoint of applications of the articular contact modelling to osteoarthritic joints. Indeed, the change of the articular cartilage thickness has been widely used as an indicator of its degenerative status.

In order to take into account the effect of energy dissipation during the elasto-plastic contact interaction, the following Hunt – Crossley equation [31] has been widely employed for modelling impact situations:

$$P(t) = b\delta_0^p(t)\dot{\delta}_0^q(t) + k\delta_0^n(t). \quad (60)$$

The stiffness coefficient k and the damping coefficient b depend on material and geometric properties of colliding bodies. As it was observed in [30], an important aspect of Eq. (60) is that damping depends on the indentation, which is physically sound since the contact area increases

with deformation and a plastic region is more likely to develop for larger contact displacements. For biomechanical applications, Eq. (60) was used in [7, 32, 33].

In the case of viscoelastic layers, according to (59), the contact constitutive relations can be represented as follows (see also, Eqs. (31) and (33)):

$$P(t) = E_\infty M R^l \int_{0-}^{t} \Psi(t-\tau) \frac{d}{d\tau}\left(\delta_0^n(\tau)\right) d\tau. \tag{61}$$

Here, E_∞ is the relaxation modulus, $\Psi(t)$ is the compound relaxation function.

It should be noted that Eqs. (59) and (61) do not exactly describe the initial short time interval of contact interaction, while the contact zone does not exceed the joint thickness of the layers. However, if the maximum characteristic size of the contact zone achieved during the loading phase is much grater than each thickness of the layers, the overall error introduced by this initial interval will be relatively small, just like it was shown in [34] with respect to the influence of the superseismic stage of contact on the Hertzian impact theory.

Observe that in contrast to Eq. (60), the force-displacement relationship (61) introduces the viscous mechanism of energy dissipation and is likely to be more physically sound in view of the biphasic nature of articular cartilage. Note also that the consideration of viscous effects in quasistatic or dynamic simulations could be important, in particular, in the simulation of total knee replacement [13].

We underline that Eqs. (59) and (61) depend on the geometrical parameters of the articular surfaces in contact, and their accurate determination is an important step in applications of these equations. In this study, we introduced the effective geometrical characteristics of articular surfaces for using in the developed asymptotic models of elliptical contact between articular surfaces.

It is interesting to observe following [5], where the effects of different mathematical descriptions of articular contact and articular surface geometry on the kinematic characteristics of the knee model were investigated, that close approximations of the articular surfaces by polynomials are not necessary, since the motion characteristics were not influenced greatly by the degree of the polynomial approximations for the curved tibial surfaces. This was caused by the size of the contact area, which covered small surface irregularities and made the contribution of the contact pressure distribution to the net contact force less dependent on the irregularities. Thus, this observation supports the necessity to operate with the effective geometrical characteristics of articular surfaces. It should be also emphasized that the analytical models for the contact force using the local geometrical characteristics (principal radii of curvature of the articular surfaces at the potential contact points P^0 and $\hat{P}^0$) in contrast to the effective geometrical characteristics are restricted to simple geometries, and therefore their applicability to real articular contact geometries is limited.

The objective of this study is to describe analytically the articular tibio-femoral contact for applications in multibody dynamic simulations of the human knee joint. As the main result of the present paper, simple asymptotic models of elliptical contact between the articular cartilage layers have been established based on the recently developed asymptotic model of frictionless elliptical contact interaction between thin biphasic or viscoelastic cartilage layers. The asymptotic models use the effective geometrical characteristics of articular surfaces, which can be determined from the introduced optimization criteria.

6 ACKNOWLEDGMENTS

The author gratefully acknowledges the financial support from the European Union Seventh Framework Programme under contract number PIIF-GA-2009-253055.

REFERENCES

[1] W. Herzog and S. Federico, Considerations on Joint and Articular Cartilage Mechanics. *Biomechanics and Modeling in Mechanobiology*, **5**, 64–81, 2006.

[2] J. Wismans, F. Veldpaus, J. Janssen, A. Huson, and P. Struben, A Three-Dimensional Mathematical Model of the Knee-Joint, *Journal of Biomechanics*, **13**, 677–679, 681–685, 1980.

[3] E.M. Abdel-Rahman and M.S. Hefzy, Three-Dimensional Dynamic Behaviour of the Human Knee Joint Under Impact Loading, *Medical Engineering & Physics*, **20**, 276–290, 1998.

[4] Z.-K. Ling, H.-Q. Guo, and S. Boersma, Analytical Study on the Kinematic and Dynamic Behaviors of a Knee Joint, *Medical Engineering & Physics*, **19**, 29–36, 1997.

[5] L. Blankevoort, J.H. Kuiper, R. Huiskes, and H.J. Grootenboer, Articular Contact in a Three-Dimensional Model of the Knee, *Journal of Biomechanics*, **24**, 1019–1031, 1991.

[6] Y. Bei and B.J. Fregly, Multibody Dynamic Simulation of Knee Contact Mechanics. *Medical Engineering & Physics*, **26**, 777–789, 2004.

[7] M. Machado, P. Flores, J.C.P. Claro, J. Ambrósio, M. Silva, A. Completo, and H.M. Lankarani, Development of a Planar Multibody Model of the Human Knee Joint, *Nonlinear Dynamics*, **60**, 459–478, 2010.

[8] J.R. Barber, Contact Problems for the Thin Elastic Layer, *International Journal of Mechanical Sciences*, **32**, 129–132, 1990.

[9] G.A. Ateshian, W.M. Lai, W.B. Zhu, and V.C. Mow, An Asymptotic Solution for the Contact of Two Biphasic Cartilage Layers, *Journal of Biomechanics*, **27**, 1347–1360, 1994.

[10] W. Wilson, C. C. van Donkelaar, R. van Rietberger, and R. Huiskes, The Role of Computational Models in the Search for the Mechanical Behaviour and Damage Mechanisms of Articular Cartilage, *Medical Engineering and Physics* **27**, 810–826, 2005.

[11] J. Z. Wu, W. Herzog and M. Epstein, Evaluation of the Finite Element Software ABAQUS for Biomechanical Modelling of Biphasic Tissues, *Journal of Biomechanics*, **31**, 165–169, 1997.

[12] D.I. Caruntu and M.S. Hefzy, 3-D Anatomically Based Dynamic Modeling of the Human Knee to Include Tibio-Femoral and Patello-Femoral joints, *Journal of Biomechanical Engineering*, **126**, 44–53, 2004.

[13] A. Pérez-González, C. Fenollosa-Esteve, J.L. Sancho-Bru, F.T. Sánchez-Marín, M. Vergara, and P.J. Rodríguez-Cervantes, A Modified Elastic Foundation Contact Model for Application in 3D Models of the Prosthetic Knee, *Medical Engineering & Physics*, **30**, 387–398, 2008.

[14] Y.-Ch. Lin, R.T. Haftka, N.V. Queipo, and B.J. Fregly, Surrogate Articular Contact Models for Computationally Efficient Multibody Dynamic Simulations, *Medical Engineering & Physics*, **32**, 584–594, 2010.

[15] I. Argatov and G. Mishuris, Elliptical Contact of Thin Biphasic Cartilage Layers: Exact Solution for Monotonic Loading, *Journal of Biomechanics*, **44**, 759–761, 2011.

[16] I. Argatov and G. Mishuris, Frictionless Elliptical Contact of Thin Viscoelastic Layers Bonded to Rigid Substrates, *Applied Mathematical Modelling*, doi:10.1016/j.apm.2011.01.029.

[17] J.H-C. Wang, J. Ryu, J.-S. Han, and B. Rowen, A New Method for the Representation of Articular Surfaces Using the Influence Surface Theory of Plates, *Journal of Biomechanics*, **33**, 629–633, 2000.

[18] R. Huiskes, R. Van Dijk, A. de Lange, H.J. Woltring, and Th.J.G. Van Rens, Kinematics of the Human Knee Joint, In: *Biomechanics of Normal and Pathological Human Articulating Joints* (N. Berme, A.E. Engin, and K.M. Correia da Silva, eds.), pp. 165–187. Martinus Nijhoff Publ., Dordrecht, 1985.

[19] Ch. Glocker, Formulation of Spatial Contact Situations in Rigid Multibody Systems, *Computer Methods in Applied Mechanics and Engineering*, **177**, 199–214, 1999.

[20] V.M. Aleksandrov and I.I. Vorovich, Contact Problems for the Elastic Layer of Small Thickness. *Journal of Applied Mathematics and Mechanics*, **28**, 425–427, 1964.

[21] K.L. Johnson, *Contact mechanics*. Cambridge Univ. Press, Cambridge, UK, 1985.

[22] M.G. Pandy, K. Sasaki, and S. Kim, A Three-Dimensional Musculoskeletal Model of the Human Knee Joint. Part 1: Theoretical Construction, *Computer Methods in Biomechanics and Biomedical Engineering*, **1**, 87–108, 1997.

[23] I.I. Argatov, The Pressure of a Punch in the Form of an Elliptic Paraboloid on a Thin Elastic Layer, *Acta Mechanica*, **180**, 221–232, 2005.

[24] R.S. Chadwick, Axisymmetric Indentation of a Thin Incompressible Elastic Layer, *SIAM Journal on Applied Mathematics*, **62**, 1520–1530, 2002.

[25] G.A. Ateshian, A B-Spline Least-Squares Surface Fitting Method for Articular Surfaces of Diarthrodial Joints, *Journal of Biomechanical Engineering*, **115**, 366–373, 1993.

[26] Y.Y. Dhaher, S.L. Delp, W.Z. Rymer, The Use of Basis Functions in Modelling Joint Articular Surfaces: Application to the Knee Joint, *Journal of Biomechanics*, **33**, 901–907, 2000.

[27] L.J. van Ruijven, M. Beek, and T.M.G.J. van Eijden, Fitting Parametrized Polynomials with Scattered Surface Data, *Journal of Biomechanics*, **32**, 715–720, 1999.

[28] S. Hirokawa, T. Ueki, and A. Ohtsuki, A New Approach for Surface Fitting Method of Articular Joint Surfaces, *Journal of Biomechanics*, **37**, 1551–1559, 2004.

[29] J. Z. Wu, W. Herzog, and M. Epstein, An Improved Solution for the Contact of two Biphasic Cartilage Layers, *Journal of Biomechanics*, **30**, 371–375, 1997.

[30] G. Gilardi and I. Sharf, Literature Survey of Contact Dynamics Modelling, *Mechanism and Machine Theory*, **37**, 1213–1239, 2002.

[31] K.H. Hunt and F.R.E. Crossley, Coefficient of Restitution Interpreted as Damping in Vibroimpact, *ASME Journal of Applied Mechanics*, **42**, 440–445, 1975.

[32] M.P.T. Silva, J.A.C. Ambrósio, and M.S. Pereira, Biomechanical Model with Joint Resistance for Impact Simulation, *Multibody System Dynamics*, **1**, 65–84, 1997.

[33] T.M. Guess, G. Thiagarajan, M. Kia, and M. Mishra, A Subject Specific Multibody Model of the Knee with Menisci, *Medical Engineering & Physics*, **32**, 505–515, 2010.

[34] I.I. Argatov, Asymptotic modeling of the impact of a spherical indenter on an elastic half-space, *International Journal of Solids and Structures*, **45**, 5035–5048, 2008.